THE JOURNAL OF PHYSICAL CHEMISTRY C

Article

pubs.acs.org/JPCC

Surface Heterogeneity of SiO_2 Polymorphs: An XPS Investigation of α-Quartz and α-Cristobalite

Cuihua Tang,[†,‡,§] Jianxi Zhu,*[,†,§] Qing Zhou,[†,‡,§] Jingming Wei,[†,§] Runliang Zhu,[†,§] and Hongping He[†,§]

[†]CAS Key Laboratory of Mineralogy and Metallogeny, Guangzhou Institute of Geochemistry, Chinese Academy of Sciences, 511 Kehua Street, Guangzhou 510640, China

[‡]University of Chinese Academy of Sciences, 19 Yuquan Road, Beijing 100049, China

[§]Key Lab of GD for Mineral Physics and Materials, 511 Kehua Street, Guangzhou 510640, China

Supporting Information

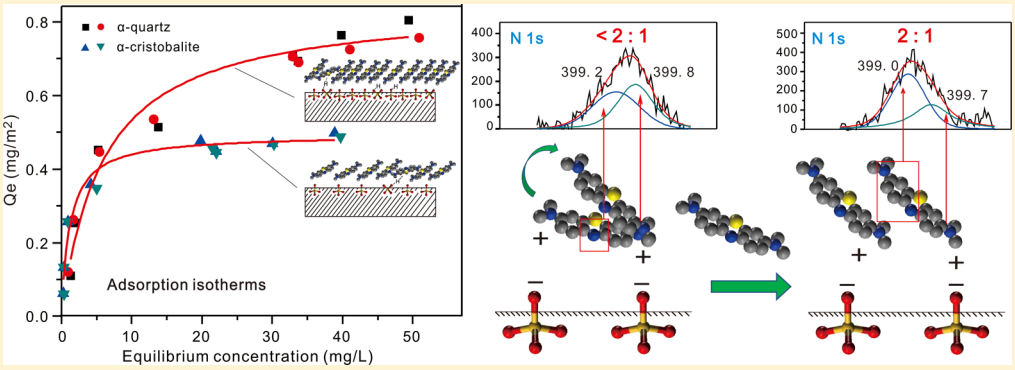

ABSTRACT: Silica minerals, one of the most abundant mineral species on the earth, play important roles in geochemistry and environment processes. The diversity of the SiO_4 tetrahedron polymerization style might result in the heterogeneity of the surface microstructures and properties of SiO_2 polymorphs. The surface properties of two common crystalline SiO_2 polymorphs, i.e., α-quartz and α-cristobalite, have been investigated by the surface site density measurement, batch methylene blue (MB) adsorption, and X-ray photoelectron spectroscopy (XPS). The Langmuir adsorption isotherms suggest the formation of monolayer MB on both α-quartz and α-cristobalite surfaces. The adsorption capacity of α-quartz toward MB is larger than that of α-cristobalite, which positively correlates with the density of surface site. XPS spectra reveal that the adsorption takes place between the nitrogen atom of the dimethylamino groups in MB and silanols on α-quartz and α-cristobalite surfaces. The O/Si atom ratio related with adsorption of α-quartz is found to be about 1.8:1, which is higher than that of α-cristobalite (about 1.3:1). This suggests that there are two different silanol species (single and germinal) related to adsorption on the surface of α-quartz and α-cristobalite, and the higher O/Si ratio implies a larger proportion of germinal silanols in α-quartz. The N_{low}/N_{high} ratio (N_{low} stands for the N atoms with lower binding energy (399.2 eV), and N_{high} for the N atoms with higher binding energy (399.7 eV)) changes to about 2:1 with the adsorption saturation, implying that the space arrangement of MB adsorbed on the surface was adjusted with the increase of adsorption amount by lifting the average tilt angle between the long axis of the MB molecule and the sample surface. The higher surface site density of α-quartz leads to a larger average tilt angle, while α-cristobalite does conversely.

1. INTRODUCTION

Silica is one of the most abundant species on the earth's crust. Because of its unique properties, silica has been wildly used in industries such as catalysis, electronic devices, optical instruments, and solar cells.[1−4] Meanwhile, as a family of significant minerals prevalent in soil, sediment, and dustfall, the silica minerals display important influences on the interface reactions during various geochemical and environmental processes.[5−8]

Crystalline silica occurs as more than 10 polymorphs with quartz, cristobalite, tridymite, coesite, stishovite, lechatelierite, chalcedony, etc. Quartz is the most common mineral in sediments and soils, and cristobalite is mainly constituted of ceramic industry dustfall. Most of silica polymorphs are composed of three-dimensional arrays of linked silicon−oxygen tetrahedrons (SiO_4), and each one has different crystal structure owning to distinct polymerization styles. The diversity of the polymerization style and the resultant minerals structures might result in the heterogeneity of the surface microstructure and properties.[9,10]

The surface hydroxyl groups, namely silanols (SiOH), are mainly responsible for the surface properties of silica minerals. A number of studies about silica surface properties have been

Received: September 15, 2014
Revised: October 21, 2014
Published: October 22, 2014

   dx.doi.org/10.1021/jp509338x | J. Phys. Chem. C 2014, 118, 26249−26257

conducted during the last decades. Legrand et al.[11] studied the silicon functionality distribution on the surface of amorphous silica by ^{29}Si solid state nuclear magnetic resonance (NMR) spectroscopy. They believed that the evolution of single versus germinal silanols was interpreted as the result of some equilibrium of the functional groups. Yuan et al.[12] further demonstrated that there are different forms of silanols existing on the diatomite (amorphous silica) surface (i.e., isolated, vicinal, germinal, and interacting via H-bond) by using ^{1}H magic-angle spinning nuclear magnetic resonance (^{1}H MAS NMR) technology. Meanwhile, a few researchers devoted themselves to point out the difference of reactivity among the various surface silanol groups. Davydov et al.[13] believed that the main role in specific adsorption and in the chemical reaction with trimethylchlorosilane must be credited to the isolated hydroxyl groups of the silica surface. However, studies centered on silica hazard and hemolytic activity[14−16] indicated the much more significant role of germinal silanols. The surface chemistry of quartz or amorphous silica, such as surface charge, complexation constants, surface silanol groups, etc., has been extensively studied by surface titration and other measurement methods.[17−19] A plethora of investigation on adsorption of quartz toward heavy metal ions has been conducted.[20] James et al.[21] thought the adsorption of Co^{2+} on quartz involved in specific adsorption, and Hayes et al.[22] supported this viewpoint with the observed phenomenon that the adsorption was effected less by the change of concentration of supporting electrolyte, while the three layers surface complexation model implied supporting electrolyte ions also participated in the reaction of surface complexation.[23] To further reveal the surface properties of different SiO_2 polymorphs, Fubini and his colleagues[24−27] investigated the heterogeneity of the surface microstructure and properties of some SiO_2 polymorphs by using water and alcohols as probe molecules via determining the adsorption enthalpy and testing hydrophilicity/hydrophobicity. Moreover, with the application of molecular simulation techniques, researchers have reported that the surface microstructures of some SiO_2 polymorphs are not in general the same,[16,28] especially in different crystal surfaces.[29−31] The difference in Si−O bond strength in silica tetrahedron results in the diverse Si−O−Si cleavage and various surface silanol groups. The distribution and density of surface silanol groups are closely related to the surface activity of silica polymorphs and crystal planes, and the different proportion of the single and germinal may lead to the diverse surface reactivity.

Because of the abundance and distinct difference in crystallinity, most of these studies paid main attention on the most common crystalline silica, namely α-quartz, as well as the amorphous phase, amorphous silica. Although a few studies on the heterogeneity of some SiO_2 polymorphs have been reported, these researches mainly focused on the interaction between the SiO_2 polymorphs and some small model molecules in a relatively simple environment. Besides the most common interaction between mineral surface and water, the interactions between mineral surface and various environment-relevant substances (particularly organic contaminants and heavy metals) also extensively exist in the earth surface environments. The interactions exert great effects on the fate of these pollutants. Although the importance of the effect of silica on the transportation and transformation of environmentally relevant substances has been realized, experimental investigation on the surface reactivity heterogeneity of several important SiO_2 polymorphs in soils or environmental system toward typical organic pollutants has been scarcely reported so far, as well as lack of reasonable reaction mechanism to interpret the interaction difference between silica polymorphs and organic molecules in a silica−water interface.

X-ray photoelectron spectroscopy (XPS) has been proven to be an efficient technique to investigate surface chemical composition of minerals such as silicates,[32−34] oxides,[35] and sulfides.[36] The surface composition of α-quartz reacted with various aqueous solutions of pH 0−10 was qualitatively and quantitatively evaluated using XPS.[37] For subtle difference among the surface properties of SiO_2 polymorphs, XPS will turn out to be a powerful tool to detect the surface heterogeneity and interpret adsorption mechanism of organic molecules under atomic level.

To further investigate the surface heterogeneity of silica polymorphs, in the present paper, the surface site density of two most common polymorphs, i.e., α-quartz and α-cristobalite, was measured by method of conventional acid−base titration. Then the performance of α-quartz and α-cristobalite in removal of typical cationic dyes methylene blue (MB) from water was investigated. In batch adsorption experiments, the adsorption amounts were obtained by examining adsorption equilibrium curves. XPS spectra of α-quartz and α-cristobalite before and after adsorption of MB were applied to determine the O/Si atomic ratio involved in adsorption and the N_{low}/N_{high} ratio (N_{low} represents nitrogen atom with the binding energy at 399.2 eV, and N_{high} represents the one with the binding energy at 399.7 eV.). With a combination of the measured surface site density, adsorption isotherms, and XPS characterization, a novel model of MB dye molecules adsorption on the silica surface is put forward.

2. EXPERIMENTAL SECTION

2.1. Materials. The natural α-quartz was collected from Guiding, Guizhou Province of China, and the commercially available α-cristobalite was purchased from Veston Silicon Co., Ltd. (Guiping County, Guangxi Province of China). Both the two samples were ground with a planetary ball mill (Fritsch Pulverisette 6, Germany) for 2 h. The powder samples were immersed in 0.01 M HCl solution for 24 h and then rinsed with deionized water until free of chloride ion. After drying, the samples were calcined in a muffle furnace at 450 °C for 12 h.

Methylene blue (MB) of reagent grade ($C_{16}H_{18}N_3SCl{\cdot}3H_2O$, purity ≥98.5%, Tianjin Kemiou Chemical Reagent Co., Ltd.) was used, without any further purification, to prepare all solutions for the experiments. The solutions were prepared with deionized water, and the pH was adjusted to 8 with standard acid (0.1 M HCl) and standard base (0.1 M NaOH) solutions. The pH value was chosen to 8 because it is the optimum pH value showed in the pre-experiments.

2.2. Characterization Techniques. The powder X-ray diffraction (XRD) measurement was conducted on a Bruker D8 Advance X-ray diffractometer, operating at 40 kV and 40 mA with Cu Kα radiation. The patterns were recorded at a 2θ range between 20° and 80° at a scanning speed of 3°/min. The reference intensity ratio (RIR) method was used for quantitative phase analysis of the selected samples.

The particle size of the powder samples was measured by laser particle size analyzer (JL-1177 full-automatic laser particle size analyzer, Chengdu, China). Nitrogen adsorption/desorption isotherms were measured at −196 °C using a Micromeritics ASAP 2020 M specific surface area and porosity

dx.doi.org/10.1021/jp509338x | J. Phys. Chem. C 2014, 118, 26249−26257

analyzer. Prior to analysis, samples were outgassed at 120 °C for 8 h. The specific surface area was calculated according to the Brunauder, Emmertt, Teller (BET) equation.

X-ray photoelectron spectroscopy analyses were carried out on a Thermo Scientific Escalab 250 instrument equipped with Al Kα source (10 mA, 14 kV) and operating at 1486.8 eV during the measurements. The base pressure in the spectrometer analyzer chamber was lower than 2×10^{-9} mbar. The charge neutralizer filament was used during all experiments to control charging of the samples. All dried mineral samples were taken to analyze as quickly as possible so that fresh and clean samples were present in all analysis. The Carbon C 1s line with a position at 284.8 eV was used as reference to correct the charging effect. Collected XPS data were analyzed with a nonlinear least-squares fit routine with Gaussian/Lorentian Area band shape.[36] All spectra were performed with Smart background correction

2.3. Surface Site Density Titration. The acid−base titration method as reported in the literature[38,39] was applied to measure the surface hydroxyl group density. Then 20 mL of standard base solution (0.1 M NaOH) was added into a dispersion of α-quartz and α-cristobalite, respectively. To make sure the reaction was performed fully, the dispersions were stirred on magnetic stirring apparatus for 12 h at room temperature. After that, the dispersions were centrifuged at 4200 rpm for 10 min. The excess base was back-titrated by standard acid solution (0.1 M HCl). All reactions and measurements were conducted at room temperature, and all the experiments were in duplicate. The average values were calculated from two independent measurements. The mole amounts of surface hydroxyl group were obtained by subtracting the consumed acid mole amounts from the total base mole amounts, and combining with the specific surface area data, the density of surface site could be calculated.

2.4. Adsorption Experiments. In adsorption experiment, certain amounts (20 g/L) of α-quartz and α-cristobalite particles were added to designated concentrations (5, 10, 20, 30, 40, 50, 60, 70 mg/L) of MB solutions, respectively. To ensure sufficient reaction space, 20 mL of solution was pushed into a 50 mL volume polypropylene centrifuge tube. Batch experiments on α-quartz and α-cristobalite were performed in an incubator shaker continuously shaking at 30 ± 2 °C with an oscillation rate of 160 rpm for 24 h. After adsorption, the dispersions were centrifuged at 4200 rpm for 15 min, and 5 mL of supernatant solutions were extracted to dilute to 25 mL solutions with deionized water. The solid samples were rinsed with deionized water and then dried in vacuum freezing dryer for 24 h. The concentrations of MB in the filtrate were determined by using ultraviolet−visible spectrophotometer (PerkinElmer Lambda 850 UV/vis spectrometer) at a wavelength of 664 nm. The determination experiments were conducted in triplicate, and the average value was taken for calculation. Blank experiments showed no detectable MB adsorbed on the surface of the centrifuge tubes. All adsorption experiments were performed in duplicate, and the results show a good repeatability. The dried samples were kept in drying apparatus for further X-ray photoelectron spectroscopy analysis.

3. RESULTS AND DISCUSSION

3.1. Sample Characterization. Powder X-ray diffraction (XRD) patterns (Figure 1) show the structural heterogeneity of the two silica polymorphs. They are identical to the international center for diffraction data (ICDD)'s powder

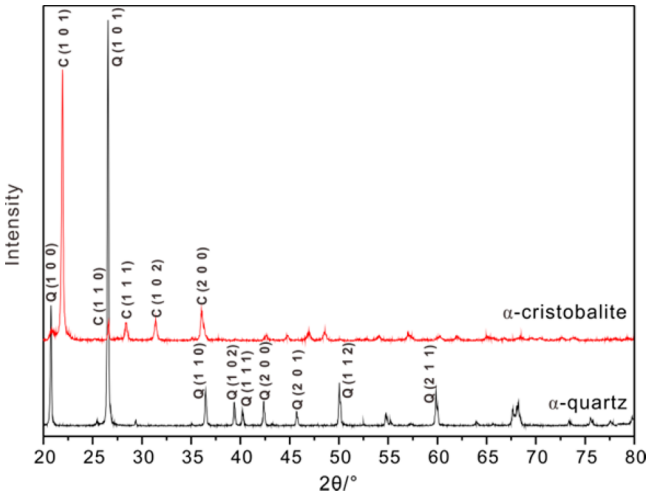

Figure 1. XRD patterns of α-quartz and α-cristobalite samples.

diffraction files (PDFs) 85−1780 and 77−1317, respectively. XRD pattern of α-quartz displays characteristic reflection at 3.35 Å (Q (101)), it belongs to trigonal, while the indicative reflection for α-cristobalite is recorded at 4.06 Å (C (101)), it belongs to tetragonal. No characteristic reflections of impurities detected in the XRD patterns of α-quartz and α-cristobalite suggests that both the two samples are of high purity. A calculation by using RIR method, a semiquantitative phase analysis technology, indicates that the purities of α-quartz and α-cristobalite are both higher than 95%.

To minimize the effect of particle size on the heterogeneity of the studied samples, both the two samples used in experiments have a similar average particle size, ca. 5 μm. The specific surface area of α-cristobalite is about 3.6 m^2/g, a slightly lower than that of α-quartz, 3.8 m^2/g. To well compare the difference of surface property between α-quartz and α-cristobalite, the amount of surface silanol groups and the adsorption capacity are both normalized to the specific surface area.

3.2. Surface Site Distribution. Generally, silica polymorphs have typical framework structure without pore and opening structures. Thus, the surface silanol groups are the predominant reactive functional groups for α-quartz and α-cristobalite. In the reaction of NaOH solution, surface silanol groups on the silica polymorphs serve as proton donators. According to the NaOH and HCl (back-titration) consumption, the total amounts of surface silanol groups could be calculated.

On the basis of acid−base titration experiments, the results indicate that the surface site density of α-quartz is 11.8 sites/nm^2, larger than that of α-cristobalite, 7.4 sites/nm^2 (Table 1). This is similar to those values of α-quartz (5−12 sites/nm^2) reported in the literature,[40,41] in which different methods were used. The reported ideal molecular computational data[29] also showed that the surface site density of α-quartz was larger than that of α-cristobalite. When compared with the computational

Table 1. Surface Site Density of α-Quartz and α-Cristobalite by Acid−Base Titration

sample	α-quartz	α-cristobalite
average surface site density (nmol/m^2)	0.0196	0.0123
surface site density (sites/nm^2)	11.8	7.4

dx.doi.org/10.1021/jp509338x | J. Phys. Chem. C 2014, 118, 26249−26257

data, both the measured values of α-quartz and α-cristobalite are larger than the computational results. This may be mainly caused by deviation in the experiments.

3.3. Adsorption Isotherms. Adsorption isotherms can illustrate the equilibrium characteristics of the adsorption of MB onto α-quartz and α-cristobalite, from which the adsorption behavior difference between adsorbate (MB) and different adsorbents (α-quartz and α-cristobalite) can be shown. In this study, the experimental data acquired at pH = 8 are well described by the linearized forms of the modified Langmuir isotherm expressed as follows:

$$\frac{C_e}{Q_e} = \frac{C_e}{Q_m} + \frac{1}{Q_m K_l}$$

where Q_e and C_e are equilibrium adsorption amount by per unit area of adsorbent and equilibrium concentration, respectively. Q_m is the saturated adsorption capacity by per unit area of adsorbent, and K_l is the Langmuir adsorption constant related to binding affinity. According to the adsorption isotherms, the adsorption mechanism of MB onto α-quartz and α-cristobalite involves in monolayer and physical adsorption. Under the condition of pH = 8, MB mainly exists in the form of cation in the solutions, and the surface of α-quartz and α-cristobalite are negatively charged because the pH of the solution is lower than their point of zero charge (pH_{pzc}). Hence, the electrostatic attraction between MB cations and the negatively charged mineral surface is the predominant interaction. Combined with the adsorbed amounts of MB and the specific surface area of α-quartz and α-cristobalite, the adsorbed amounts of MB on per unit area of the samples can be calculated. Also, the related adsorption constants are obtained from the adsorption isotherms (Figure 2) and presented in the Supporting Information, Table S1.

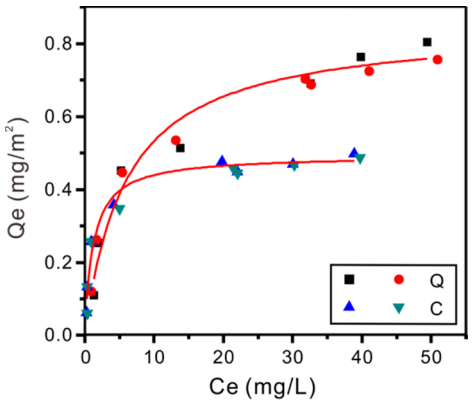

Figure 2. Adsorption isotherms for MB adsorption by α-quartz (Q) and α-cristobalite (C). Independent experiments of α-quartz or α-cristobalite were conducted in duplicate, and the fitting curves were fitted as one of the set of data, respectively.

The adsorbed amounts increase with the increasing initial concentrations of MB solution until reaching a maximum (Figure 2). The maximum of adsorbed MB on per unit area of α-quartz is significantly larger than that of α-cristobalite. As depicted in the plot, at a relatively lower initial concentration (<6 mg/L), more MB cations are adsorbed on per unit area of α-cristobalite than that of α-quartz. However, when the equilibrium concentration is above 6 mg/L, the amounts of adsorbed MB by α-quartz become obviously larger than that by α-cristobalite. Our calculation based on the surface acid−base titration results demonstrates that the density of surface hydroxyl groups of α-quartz (11.8 sites/nm^2) is larger than that of α-cristobalite (7.4 sites/nm^2). Correspondingly, the saturated MB adsorption amount by α-quartz (0.85 mg/m^2) is higher than that of α-cristobalite (0.49 mg/m^2). The difference of adsorption maximum between α-quartz and α-cristobalite should be attributed to the nature, density, and distribution of surface silanol groups. The effect of surface silanol groups density on adsorption is remarkable,[42] i.e., sufficient space is needed for the array of the adsorbed MB. The space requirement for a MB monomer is significantly larger than that available for a single metal ion as mentioned in ref 43. Because of the close distance between two vicinal hydroxyl group sites, once one site is bonded with adsorbate cations, the other may be subject to be sheltered by the free end of the adsorbed monomer, forming a temporarily invalid reactive site.[44] Compared with α-quartz, α-cristobalite has a smaller silanol density. Thus, at the first stage, the adsorption amount of α-cristobalite per unit area is larger than that of α-quartz. With the increasing of the MB concentrations, the adsorbed MB undergoes reorientation,[42,45] and subsequently with the adjustment of monomer arrangement, temporarily invalid reactive sites become available, resulting in an increase of adsorbed MB amount until a saturation state (adsorption maximum). That is to say, the saturated adsorption amount of α-quartz becomes larger than that of α-cristobalite, resulting from the different surface silanol groups density. As we all know, the most common types of SiOH on silica polymorphs are isolated, germinal, vicinal, and so on. In a sense, germinal silanol is a kind of particular vicinal silanol, which has a remarkable effect on the adsorption behavior of SiO_2 polymorphs. Previous work[16] has suggested that silica surface reactivity has a direct relationship with the density of germinal silanols. Significantly, although it is tough to directly measure the amount of germinal silanols due to the sensitivity limit of determination techniques, there are still some clues on the difference of distribution of germinal silanols on α-quartz and α-cristobalite in our following work.

3.4. X-ray Photoelectron Spectroscopy. XPS is an effective method to investigate the interaction between mineral surface and MB as well as the chemical states of MB adsorbed on the surface.[43] On the basis of survey scan, the emission lines of relevant elements, such as oxygen, silicon, and nitrogen, have been analyzed carefully. The content of sulfur in the MB-adsorbed samples is very low (0.2−0.4 atomic percent). At the same time, the signals corresponding to carbon are very complicated and it is difficult to give accurate assignments. Thus, the two elements (i.e., S and C) were not discussed in the paper.

XPS spectra and the best fit of oxygen regions for the samples before and after adsorption of MB are shown in Figure 3 and the Supporting Information, Table S2. According to the previous studies,[37,46,47] an O species at 531.5 eV observed on α-quartz was assigned to the O atoms in the interface Si−O−M (M represents reactive site on adsorbate). This lower binding energy is responsible for the negative shift of the enveloping peak of the samples with MB (Figure 3). The binding energies of the bulk oxygen atoms (Si−O−Si) and the surface oxygen atoms of silanols (Si−O−H) are very close, centered at 532.5 and 532.0 eV, respectively.[37,47] Additionally, a possible deviation between two independent experiments can reach 0.1−0.2 eV, which makes it harder to separate the two signals.

dx.doi.org/10.1021/jp509338x | J. Phys. Chem. C 2014, 118, 26249−26257

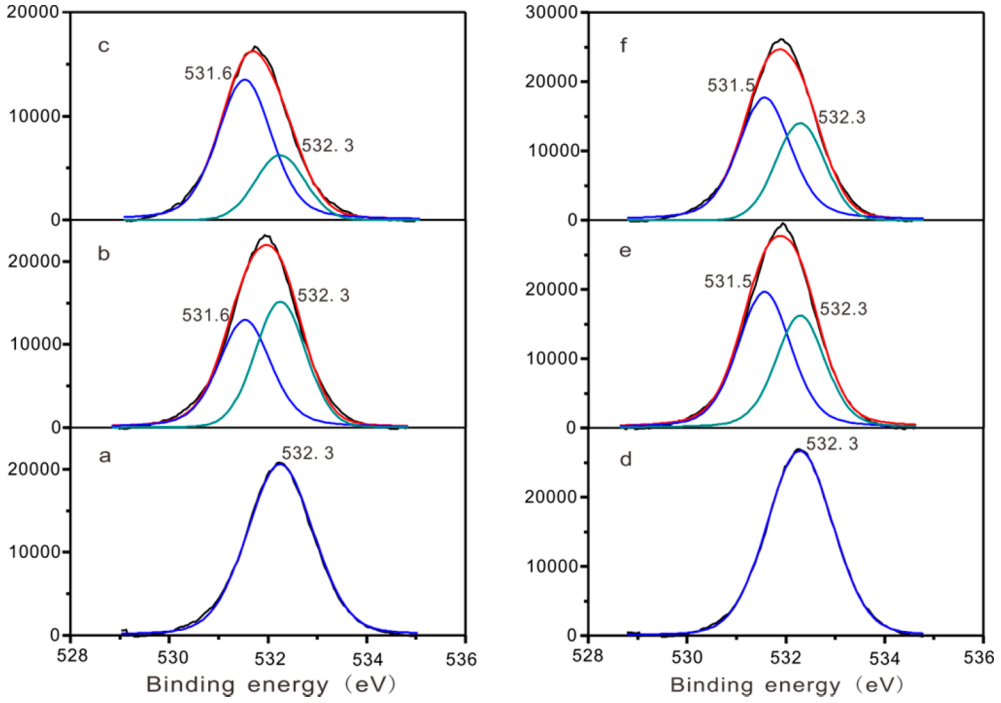

Figure 3. XPS spectra of the O 1s lines of α-quartz (a), α-quartz with unsaturated MB adsorption (b), α-quartz with saturated MB adsorption (c), α-cristobalite (d), α-cristobalite with unsaturated MB adsorption (e), α-cristobalite with saturated MB adsorption (f).

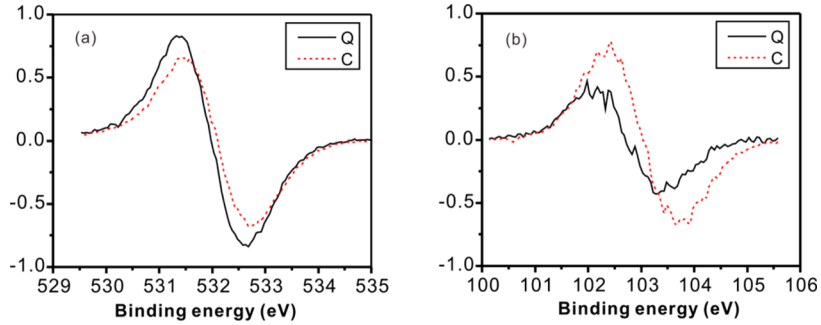

Figure 4. O 1s (a) and Si 2p (b) lines of α-quartz (Q) and α-cristobalite (C) after subtraction from MB-adsorbed adsorbents to fresh adsorbents.

Because the intensity of the two signals keeps a consistent changing tendency, the O 1s peaks of siloxane bridges (Si−O−Si) and hydroxyl groups (Si−O−H) was merged into one enveloping peak in the best fit of O 1s region, centered at 532.3 eV, as depicted in plot of α-quartz (Figure 3a) and α-cristobalite (Figure 3d). The position of the whole broad O 1s line shifts to lower binding energy gradually with increasing of the adsorbed MB amounts for both α-quartz and α-cristobalite. The negative shifts imply the changes in the local environment of surface oxygen atoms from neutral to more electronegative. On one hand, the point of zero charge (PZC) of silica is close to pH = 3, and the pH in the experiment is about 8. The relatively high pH in the experiments will result in deprotonation reaction of α-quartz and α-cristobalite surface silanol groups as follows:[19]

$$>SiOH + OH^- \Rightarrow SiO^- + H_2O$$

$$>SiO^- + M^+ \Rightarrow SiOM$$

The adsorption of MB cations promotes the O 1s signal intensity of surface hydroxyl group to decrease and the signal intensity of interface oxygen atoms attributing to Si−O−M to increase. On the other hand, the probing depth of XPS is about 15 Å, namely thickness of 7−8 atoms. The signal intensity of O 1s assigning to bulk oxygen atoms (Si−O−Si) will be weakened due to the thicker adsorption layer. For monolayer adsorption model, thickness of adsorption layer is governed by geometrical arrangement of monomers adsorbed on the surface. More detailed information about space array of MB on α-quartz and α-cristobalite will be interpreted in the part of adsorption model.

At the same time, silicon is another atom that can provide useful information about surface characteristics of α-quartz and α-cristobalite. All the Si 2p lines of the samples with different amounts of adsorbed MB show a negative shift when compared with those of α-quartz and α-cristobalite before adsorption (Supporting Information, Figure S3, Table S4). This is similar to the change on O 1s lines of the two minerals before and after adsorption of MB. This shift is caused by the lower binding energy peak at 102.6 eV because of the adsorption of MB onto the surface of α-quartz and α-cristobalite. The Si 2p region exhibits a peak with a binding energy of 103.1 or 103.2 eV, which is typical for a Si^{4+} oxidation state.[48] To clearly display the difference between the Si 2p lines before and after

dx.doi.org/10.1021/jp509338x | J. Phys. Chem. C 2014, 118, 26249−26257

adsorption of MB, the spectra have been background subtracted, normalized, and then subtracted from MB-adsorbed absorbents to the fresh ones, and so have the O 1s spectra.[35]

For quantitative evaluation of the surface adsorption site species, the subtraction spectra of O 1s and Si 2p lines before and after adsorption of MB are shown in Figure 4. The shift differences of O 1s and Si 2p lines between α-quartz and α-cristobalite will be apparent from the spectra. The plots clearly show that the intensity of the lower binding energy of O 1s and Si 2p lines increases with MB adsorption for both α-quartz and α-cristobalite, which indicates the increasing amounts of surface sites interacting with MB. It is noteworthy that the atomic ratio of the surface oxygen atoms reacting with MB (Si−O−M) to the surface silicon atoms bonding to the former oxygen atoms (Si−O−M) suggests the difference between α-quartz and α-cristobalite. The proportion of the part over zero graduation line is quantified as the atomic ratio. The O/Si atomic ratio for α-quartz is about 1.8:1, completely identical with that of the referred paper,[37] and the ratio is larger than that of α-cristobalite, about 1.3:1. Their surface O/Si atomic ratios are both between 1:1 (isolated hydroxyls) and 2:1 (germinal hydroxyls), suggesting that there are two different silanol species on the surface of α-quartz and α-cristobalite. Moreover, the higher O/Si atomic ratio in α-quartz implies the higher proportion of germinal silanols.

MB is a kind of typical cationic dye, in which the positive charge is equally stabilized in the whole molecule owning to the π* resonance. Once the π* resonance is destroyed, the positive charge will be reallocated on the nitrogen atoms of the dimethylamino groups (Figure 5). When the reallocation of positive charge is induced by negative charge, or other forces, the distribution of positive charge will display inequality.[43]

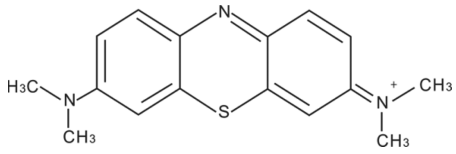

Figure 5. Schematic model of MB cation.

The N 1s lines also show pronounced difference between nitrogen atoms in pure MB bulk and that adsorbed on α-quartz and α-cristobalite (Figure 6). The N 1s emission line in the bulk shows a narrow and symmetric peak at 399.2 eV with a fwhm of 1.4 eV, indicating that the chemical environments of all nitrogen atoms are identical.[45] Upon adsorption, these lines become significantly broader and exhibit a shoulder at higher binding energy at about 399.7 eV. A shift to higher binding energy for one of the nitrogen atoms indicates a corresponding decrease in the electron density for the N atoms. The higher shift can be interpreted as a stabilization of the positive charge for MB at one of the nitrogen atoms of the dimethylamino groups in the adsorbed state on the surface. Slight shifts toward lower binding energy for the other two N atoms are also observed due to a slight increase of electron density than in the bulk state. In the best fit of nitrogen regions, the two species in different atomic environment located at 399.2 eV (N_{low}) and 399.7 eV (N_{high}) could be separated. The detailed information about the N 1s lines (e.g., fwhm) is shown in Table 2. The stoichiometric ratio of the two components (N_{low}/N_{high}) increases to about 2:1 with the adsorption amounts of MB climbing up to the maximum. This implies that geometric

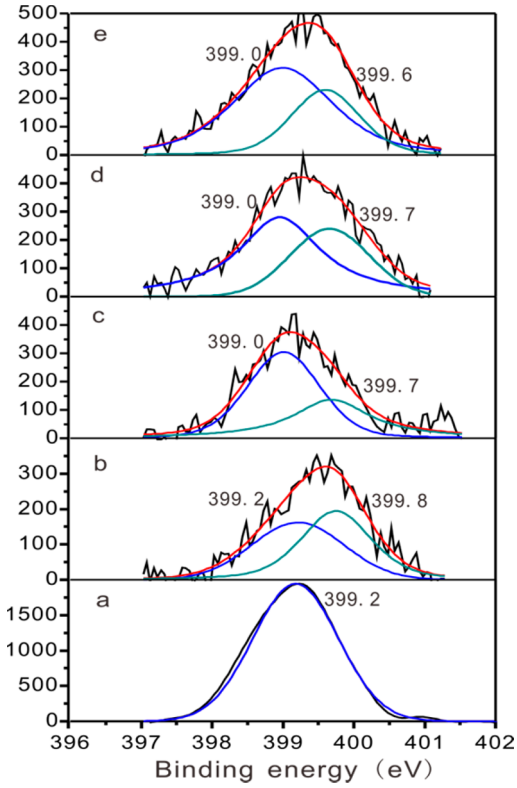

Figure 6. XPS spectra of the N 1s lines of pure methylene blue (MB) powder (a), α-quartz with unsaturated MB adsorption (b), α-quartz with saturated MB adsorption (c), α-cristobalite with unsaturated MB adsorption (d), α-cristobalite with saturated MB adsorption (e).

Table 2. Chemical Composition of N for MB Bulk Sample and Adsorbed on α-Quartz and α-Cristobalite

	binding energy (eV)	fwhm (eV)	distribution (%)	N_{low}/N_{high}	standard deviation R^2
MB	399.2	1.4	100		0.996
Q-1	399.2	1.5	50.3	1.01:1	0.941
	399.8	1.2	49.7		
Q-2	399.0	1.2	64.3	1.81:1	0.929
	399.7	1.3	35.7		
C-1	399.0	1.4	59.0	1.44:1	0.957
	399.7	1.3	41.0		
C-2	399.0	1.7	66.1	1.95:1	0.969

arrangement of MB monomers is adjusted with an increase of the adsorbed MB amounts. The stabilization of adsorbed molecules on the mineral surface is comprised of electrostatic attraction, electrostatic repulsion of neighboring monomers, van der Waals Force, and so on. When the mineral surface space is enough to hold the adsorbed monomers, the MB monomers tend to contact with the surface by a larger area. Additionally, the extra electronegative surface site will interact with the other electropositive nitrogen atoms of the dimethylamino groups of the adsorbed MB, while the inequality in the distribution of positive charge on the nitrogen atoms of the dimethylamino groups will result in the active force is much weaker. When other invading MB gets close to surface, the

dx.doi.org/10.1021/jp509338x | J. Phys. Chem. C 2014, 118, 26249−26257

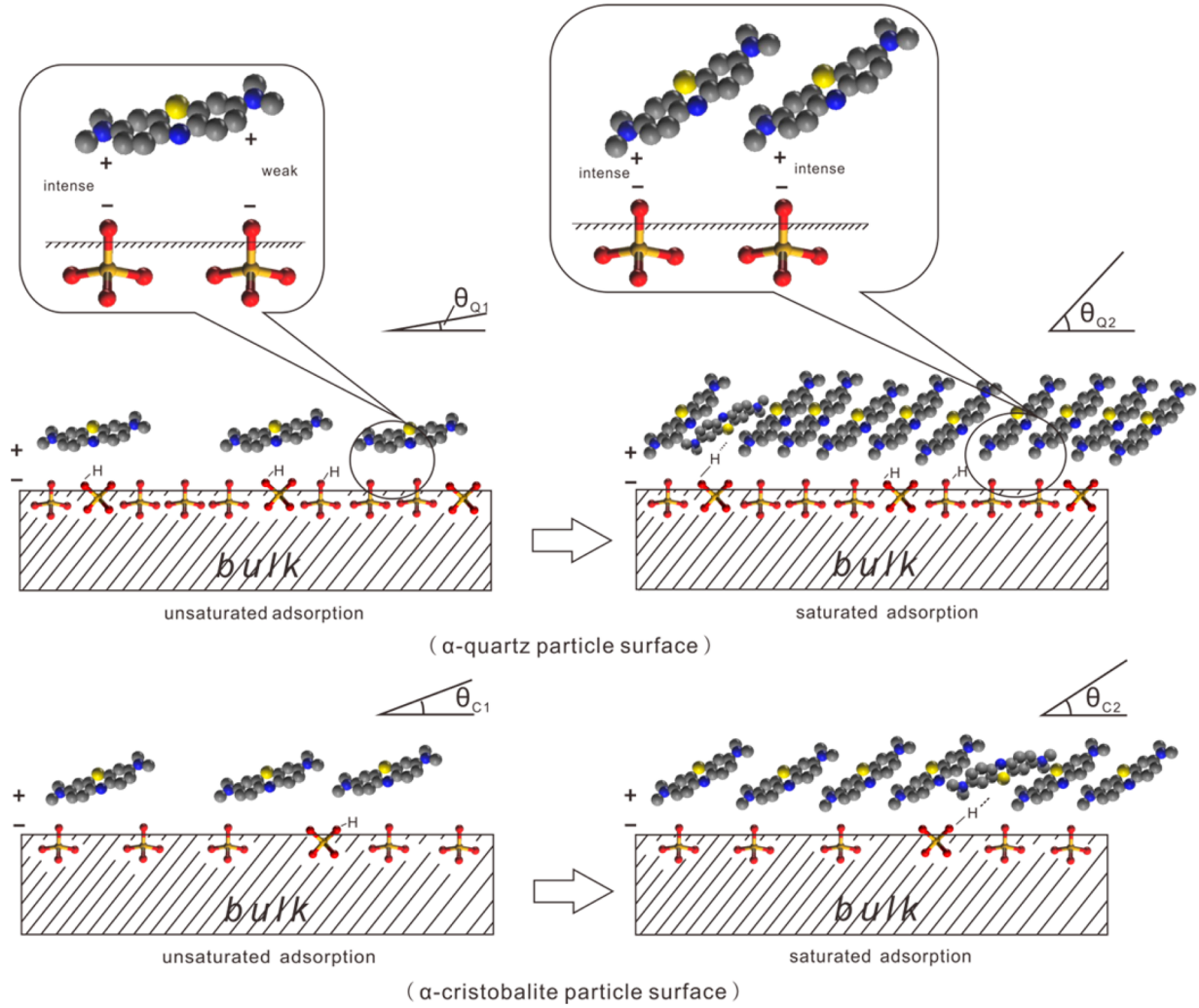

Figure 7. Schematic drawing of adsorption process of MB on α-quartz and α-cristobalite; θ_{Q1}, θ_{Q2}, θ_{C1}, and θ_{C2} represent the average tilt angle between the long axis of the MB monomer and α-quartz and α-cristobalite surface, respectively; 1 represents the unsaturated state, and 2 represents the saturated state ($\theta_{Q1} < \theta_{Q2}$, $\theta_{C1} < \theta_{C2}$, $\theta_{Q1} < \theta_{C1}$).

weaker interaction may be broken by the stronger electrostatic attraction between surface sites and MB. The integrated force may lead their average tilt angle upraising. Subsequently, the temporarily invalid silanols are exposed and turn into active ones. In a way, the more MB adsorbed, the larger their average tilt angle. However, even with roughly equal load per unit area for the unsaturated states, the N_{low}/N_{high} ratio of α-quartz is a bit lower than that of α-cristobalite. This also can be explained by the fact that the surface site density of α-quartz is larger, and more extra electronegative surface sites are available. The nitrogen atoms in the dimethylamino groups on the free end of MB are easier to be attracted by the electrostatic force, resulting in the adsorbed MB on the surface of α-quartz with lower average tilt angle. The schematic drawing of adsorption process of MB onto α-quartz and α-cristobalite, and the different behavior resulted from their surface heterogeneity are depicted in Figure 7.

3.5. Adsorption Model. The schematic drawing (Figure 7) describes an ideal adsorption process, which is modeled for a more complicated actual situation. The schematic drawing clearly displays the changes in average geometric distribution of MB adsorbed on α-quartz and α-cristobalite from the unsaturated state to the saturated one. There is some difference between α-quartz and α-cristobalite even though they own roughly equal adsorption amounts (the left part in Figure 7). This can be interpreted by the effect of the density of surface sites. In the case of α-quartz with saturated adsorption, the larger surface site density keeps larger average tilt angle due to the weak interaction between free end of the adsorbed MB and surface site. The average tilt angle between the long axis of the MB molecule and the mineral surface can be obtained from the following equation:

$$\cos\theta = \frac{1/(m \times N_A/M_{MB})}{S_{MB}}$$

Where θ (deg) is the average tilt angle, and m (mg/m^2) is the adsorption amount per unit area, N_A is the Avogadro constant, M_{MB} is the relative molecular mass of MB, and S_{MB} (Å^2) is the area of MB monomer on a flat orientation (125 Å^2).[43] Thus, combining with the adsorption amount per unit area of α-quartz (0.85 mg/m^2) and α-cristobalite (0.49 mg/m^2), we can roughly evaluate their average tilt angles θ_Q and θ_C at approximately 60° and 30°, respectively.

dx.doi.org/10.1021/jp509338x | J. Phys. Chem. C 2014, 118, 26249−26257

$$\cos\theta_Q = (1/(0.85 \times 10^{-3} \times 6.02 \times 10^{23}/319.9 \times 10^{20}))/125, \quad \theta_Q \approx 60.0°$$

$$\cos\theta_C = (1/(0.49 \times 10^{-3} \times 6.02 \times 10^{23}/319.9 \times 10^{20}))/125, \quad \theta_C \approx 29.8°$$

The average tilt angle for α-cristobalite (θ_C) with a saturated adsorption of MB is about 30°, very different from that of α-quartz (θ_Q). Interestingly, the average tilt angle for α-cristobalite is similar to that of vitreous silica as reported in the literature,[49] confirming the similarity in the surface site density and surface reactivity.[14,16] However, we could not get much more quantitative details about the reactivity difference between single and germinal silanols on α-quartz and α-cristobalite in the present study, which is of high importance for better understanding the surface heterogeneity of silica polymorphs and under way by using molecular simulation.

4. CONCLUSION

In this study, the surface heterogeneity of α-quartz and α-cristobalite are investigated by acid−base titration, adsorption experiments, and XPS spectroscopy. Acid−base titration result shows that the surface site density of α-quartz is higher than that of α-cristobalite, which significantly affects their adsorption performance toward MB. At low initial concentration, more MB is adsorbed on per unit area of α-cristobalite than on that of α-quartz. With increasing of the concentration, the amount of adsorbed MB on α-quartz becomes larger than that of α-cristobalite. The interaction between SiO_2 polymorphs (i.e., α-quartz and α-cristobalite) surface and MB mainly involves electrostatic attraction between surface hydroxyl groups and nitrogen atom of the dimethylamino groups of MB. The atomic ratio of the total surface oxygen reacting with MB to the total surface silicon bonding to the former oxygen (O/Si) is indicative of the proportions of single and germinal silanols on α-quartz and α-cristobalite surface. For the first time, it is demonstrated that the O/Si atomic ratio of α-quartz is higher than that of α-cristobalite by experiment, i.e., α-quartz has a higher proportion of germinal silanols than α-cristobalite. On the other hand, the XPS spectra show that the stoichiometric ratio of N_{low}/N_{high} reaches about 2:1as the adsorption achieves the saturation. The change of the N_{low}/N_{high} ratio reflects that the arrangement of MB monomers on surface can be adjusted in the adsorption process by lifting of average tilt angle between the long axis of the MB and samples surface.

The present study clearly reveals surface heterogeneity of SiO_2 polymorphs by experimental ways. As one of the most abundant mineral species on the earth, the obtained insights are of high importance for better understanding the role of silica minerals in various environments and their industrial application.

■ ASSOCIATED CONTENT

Supporting Information

Isotherm constants for adsorption of MB onto α-quartz and α-cristobalite; chemical composition of O for MB bulk sample and adsorbed on α-quartz and α-cristobalite; XPS spectra of the Si 2p lines of α-quartz and α-cristobalite; chemical composition of Si for MB bulk sample and adsorbed on α-quartz and α-cristobalite. This material is available free of charge via the Internet at http://pubs.acs.org.

■ AUTHOR INFORMATION

Corresponding Author

*E-mail: zhujx@gig.ac.cn.

Notes

The authors declare no competing financial interest.

■ ACKNOWLEDGMENTS

This work was supported by the National Natural Science Foundation of China (grant 41073084). This is a contribution (no. IS-1968) from GIGCAS.

■ REFERENCES

(1) Fyfe, W. S.; McKay, D. S. Hydroxyl Ion Catalysis of Crystallization of Amorphous Silica at 330 °C and Some Observations on Hydrolysis of Albite Solutions. *Am. Mineral.* **1962**, *47*, 83−89.

(2) Hopkinson, L.; Roberts, S.; Herrington, R.; Wilkinson, J. The Nature of Crystalline Silica from the TAG Submarine Hydrothermal Mound, 26° N Mid Atlantic Ridge. *Contrib. Mineral. Petrol.* **1999**, *137*, 342−350.

(3) Gerasimova, N. G. CaF_2, MgF_2, SiO_2, Al_2O_3, SiC, LiF, BaF_2, and ZrO_2 Optical Single Crystals Used in Studies in the VUV Spectral Region. *Instrum. Exp. Technol.* **2006**, *49*, 408−412.

(4) Hwang, S. H.; Shin, D. H.; Yun, J.; Kim, C.; Choi, M.; Jang, J. SiO_2/TiO_2 Hollow Nanoparticles Decorated with Ag Nanoparticles: Enhanced Visible Light Absorption and Improved Light Scattering in Dye-Sensitized Solar Cells. *Chemistry (Weinheim, Germany)* **2014**, *20*, 4439−4446.

(5) Bakos, T.; Rashkeev, S. N.; Pantelides, S. T. Reactions and Diffusion of Water and Oxygen Molecules in Amorphous SiO_2. *Phys. Rev. Lett.* **2002**, *88*, 055508.

(6) James, R. O.; Healy, T. W. Adsorption of Hydrolyzable Metal Ions at the Oxide−Water Interface. II. Charge Reversal of SiO_2 and TiO_2 Colloids by Adsorbed Co (II), La (III), and Th (IV) as Model Systems. *J. Colloid Interface Sci.* **1972**, *40*, 53−64.

(7) Freedman, Y. E.; Magaritz, M.; Long, G. L.; Ronen, D. Interaction of Metal with Mineral Surfaces in a Natural Groundwater Environment. *Chem. Geol.* **1994**, *116*, 111−121.

(8) Wang, J.; Mao, B.; White, M. G.; Burda, C.; Gole, J. L. Interactive Metal Ion−Silicon Oxidation/Reduction Processes on Fumed Silica. *RSC Adv.* **2012**, *2*, 10209−10216.

(9) Wang, P.; Pan, Z. L.; Weng, L. B. *Systermatic Mineralogy*; Geology Publisher: Beijing, 1982; 504−515.

(10) Koretsky, C. M.; Sverjensky, D. A.; Sahai, N. A Model of Surface Site Types on Oxide and Silicate Minerals Based on Crystal Chemistry; Implications for Site Types and Densities, Multi-Site Adsorption, Surface Infrared Spectroscopy, and Dissolution Kinetics. *Am. J. Sci.* **1998**, *298*, 349−438.

(11) Legrand, A.; Taïbi, H.; Hommel, H.; Tougne, P.; Leonardelli, S. Silicon Functionality Distribution on the Surface of Amorphous Silicas by ^{29}Si Solid State NMR. *J. Non-Cryst. Solids* **1993**, *155*, 122−130.

(12) Yuan, P.; Wu, D. Q.; Chen, Z.; Chen, Z. W.; Lin, Z. Y.; Diao, G. Y.; Peng, J. L. ^1H MAS NMR Spectra of Hydroxyl Species on Diatomite Surface. *Chin. Sci. Bull.* **2001**, *46*, 1112−1115.

(13) Davydov, V. YA.; Kiselev, A. V.; Zhuravlev, L. T. Study of the Surface and Bulk Hydroxyl Groups of Silica by Infrared Spectra and D_2O Exchange. *Trans. Faraday Soc.* **1964**, *60*, 2254−2264.

(14) Stalder, K.; Stöber, W. Haemolytic Activity of Suspensions of Different Silica Modifications and Inert Dusts. *Nature* **1965**, *207*, 874−875.

(15) Nash, T.; Allison, A. C.; Haringto, J. S. Physico-Chemical Properties of Silica in Relation to Its Toxicity. *Nature* **1966**, *210*, 259−261.

(16) Murashov, V.; Harper, M.; Demchuk, E. Impact of Silanol Surface Density on the Toxicity of Silica Aerosols Measured by Erythrocyte Haemolysis. *J. Occup. Environ. Hyg.* **2006**, *3*, 718−723.

(17) Wu, H. H.; Wu, D. Q.; Peng, J. L. Experimental Study on Surface Reactions of Heavy Metal Ions with Quartz. *Geochimica* **1998**, *27*, 523−531.
(18) Manceau, A.; Schlegel, M.; Nagy, K. L.; Charlet, L. Evidence for the Formation of Trioctahedral Clay upon Sorption of Co^{2+} on Quartz. *J. Colloid Interface Sci.* **1999**, *220*, 181−197.
(19) Pokrovsky, O. S.; Golubev, S. V.; Mielczarski, J. A. Kinetic Evidences of the Existence of Positively Charged Species at the Quartz−Aqueous Solution Interface. *J. Colloid Interface Sci.* **2006**, *296*, 189−194.
(20) O'Day, P. A.; Chisholm-Brause, C. J.; Towle, S. N.; Parks, G. A.; Brown, G. E. X-Ray Absorption Spectroscopy of Co(II) sorption complexes on quartz (α-SiO_2) and rutile (TiO_2). *Geochim. Cosmochim. Acta* **1996**, *60*, 2515−2532.
(21) James, R. O.; Healy, T. W. Adsorption of Hydrolyzable Metal Ions at the Oxide/Water Interface. I. Co (II) Adsorption on SiO_2 and TiO_2 as Model Systerms. *J. Colloid Interface Sci.* **1978**, *40*, 42−52.
(22) Hayes, K. F.; Leckie, J. O. Modeling Ionic-Strength Effects on Cation Adsorption at Hydrous Oxide−Solution Interface. *J. Colloid Interface Sci.* **1987**, *115*, 564−572.
(23) Katz, L. E.; Hayes, K. F. Surface Complexation Modeling. I. Strategy for Modeling Monomer Complex Formation at Moderate Surface Coverage. *J. Colloid Interface Sci.* **1995**, *170*, 477−490.
(24) Bolis, V.; Fubini, B.; Coluccia, S.; Mostacci, E. Surface Hydration of Crystalline and Amorphous Silicas. *J. Therm. Anal. Calorim.* **1985**, *30*, 1283−1292.
(25) Bolis, V.; Fubini, B.; Giamello, E. Effect of Form on the Surface Chemistry of Finely Divided Solids. *Mater. Chem. Phys.* **1991**, *29*, 153−164.
(26) Fubini, B.; Bolis, V.; Cavenago, A.; Garrone, E.; Ugliengo, P. Structural and Induced Heterogeneity at the Surface of Some SiO_2 Polymorphs from the Enthalpy of Adsorption of Various Molecules. *Langmuir* **1993**, *9*, 2712−2720.
(27) Bolis, V.; Cavenago, A.; Fubini, B. Surface Heterogeneity on Hydrophilic and Hydrophobic Silicas: Water and Alcohols as Probes for H-Bonding and Dispersion Forces. *Langmuir* **1997**, *13*, 895−902.
(28) Bourova, E.; Parker, S. C.; Richet, P. High-Temperature Structure and Dynamics of Coesite (SiO_2) from Numerial Simulations. *Phys. Chem. Miner.* **2004**, *31*, 569−579.
(29) Murashov, V. V.; Demchuk, E. Surface Sites and Unrelaxed Surface Energies of Tetrahedral Silica Polymorphs and Silicate. *Surf. Sci.* **2005**, *595*, 6−19.
(30) Tielens, F.; Gervais, C.; Lambert, J. F.; Mauri, F.; Costa, D. Ab Initio Study of the Hydroxylated Surface of Amorphous Silica: A Representative Model. *Chem. Mater.* **2008**, *20*, 3336−3344.
(31) Musso, F.; Sodupe, M.; Corno, M.; Ugliengo, P. H-Bond Features of Fully Hydroxylated Surfaces of Crystalline Silica Polymorphs: A Periodic B3LYP Study. *J. Phys. Chem. C* **2009**, *113*, 17876−17884.
(32) Gier, S.; Johns, W. D. Heavy Metal Adsorption on Micas and Clay Minerals Studied by X-Ray Photoelectron Spectroscopy. *Appl. Clay Sci.* **2000**, *16*, 289−299.
(33) Torres Sánchez, R. M.; Genet, M. J.; Gaigneaux, E. M.; dos Santos Afonso, M.; Yunes, S. Benzimidazole Adsorption on the External and Interlayer Surfaces of Raw and Treated Montmorillonite. *Appl. Clay Sci.* **2011**, *53*, 366−373.
(34) Sun, Z. M.; Bai, C. H.; Zheng, S. L.; Yang, X. P.; Frost, R. L. A Comparative Study of Different Porous Amorphous Silica Mineral Supported TiO_2 Catalysts. *Appl. Catal., A* **2013**, *458*, 103−110.
(35) Chowdhury, S. R.; Yanful, E. K.; Pratt, A. R. Chemical States in XPS and Raman Analysis During Removal of Cr(VI) from Contaminated Water by Mixed Maghemite−Magnetite Nanoparticles. *J. Hazard. Mater.* **2012**, *235*, 246−256.
(36) Gilles, E. J.; Bancroft, G. M. An XPS and SEM Study of Gold Deposition at Low Temperatures on Sulphide Mineral Surfaces: Concentration of Gold by Adsorption/Reduction. *Geochim. Cosmochim. Acta* **1985**, *49*, 979−987.
(37) Duval, Y.; Mielczarski, J. A.; Pokrovsky, O. S.; Mielczarski, E.; Ehrhardt, J. J. Evidence of the Existence of Three Types of Species at the Quartz−Aqueous Solution Interface at pH 0−10: XPS Surface Group Quantification and Surface Complexation Modeling. *J. Phys. Chem. B* **2002**, *106*, 2937−2945.
(38) Hohl, H.; Stumm, W. Interaction of Pb^{2+} with Hydrous γ-Al_2O_3. *J. Colloid Interface Sci.* **1976**, *55*, 281−288.
(39) Meder, F.; Kaur, S.; Treccani, L.; Rezwan, K. Controlling Mixed-Protein Adsorption Layers on Colloidal Alumina Particles by Tailoring Carboxyl and Hydroxyl Surface Group Densities. *Langmuir* **2013**, *29*, 12502−12510.
(40) Yates, D. E.; Grieser, F.; Cooper, R.; Healy, T. W. Tritium Exchange Studies on Metal Oxide Colloidal Dispersions. *Aust. J. Chem.* **1977**, *30*, 1655−1660.
(41) Riese, A. C..Adsorption of radium and thorium onto quartz and kaolinite: a comparison of solution/surface equilibria models. Colorado School of Mines: Golden, CO, 1982.
(42) Marucco, A.; Turci, F.; O'Neill, L.; Byrne, H. J.; Fubini, B.; Fenoglio, I. Hydroxyl Density Affects the Interaction of Fibrinogen with Silica Nanoparticles at Physiological Concentration. *J. Colloid Interface Sci.* **2014**, *419*, 86−94.
(43) Hähner, G.; Marti, A.; Spencer, N. D.; Caseri, W. R. Orientation and Electronic Structure of Methylene Blue on Mica: A Near Edge X-Ray Absorption Fine Structure Spectroscopy Study. *J. Chem. Phys.* **1996**, *104*, 7749−7757.
(44) Fisk, J. D.; Batten, R.; Jones, G.; O'Reill, J. P.; Shaw, A. M. pH Dependence of the Crystal Violet Adsorption Isotherm at the Silica−Water Interface. *J. Phys. Chem. B* **2005**, *109*, 14475−14480.
(45) Fischer, D.; Caseri, W. R.; Hähner, G. Orientation and Electronic Structure of Ion Exchanged Dye Molecules on Mica: An X-ray Absorption Study. *J. Colloid Interface Sci.* **1998**, *198*, 337−346.
(46) Weissenrieder, J.; Kaya, S.; Lu, J. L.; Gao, H. J.; Shaikhutdinov, S.; Freund, H. J.; Sierka, M.; Todorova, T. K.; Sauer, J. Atomic Structure of a Thin Silica Film on a Mo (112) Substrate: A Two-Dimensional Network of SiO_4 Tetrahedra. *Phys. Rev. Lett.* **2005**, *95*, 076103.
(47) Kaya, S.; Weissenrieder, J.; Stacchiola, D.; Shaikhutdinov, S.; Freund, H. J. Formation of an Ordered Ice Layer on a Thin Silica Film. *J. Phys. Chem. C* **2007**, *111*, 759−764.
(48) Moulder, J. F.; Stickle, W. F.; Sobol, P. E.; Bomben, K. D. *Handbook of X-ray Photoelectron Spectroscopy*; Perkin-Elmer Corporation: Eden Prairie, MN, 1992; pp 52−53.
(49) Higgins, D. A.; Byerly, S. K.; Abrams, M. B.; Corn, R. M. Second Harmonic Generation Studies of Methylene Blue Orientation at Silica Surfaces. *J. Phys. Chem.* **1991**, *95*, 6984−6990.

NOTE ADDED AFTER ASAP PUBLICATION

This paper was published ASAP on November 5, 2014, without all of the author's final corrections applied. The complete, corrected version was reposted on November 13, 2014.